Journal of Achievements in Materials and Manufacturing Engineering
VOLUME 38
ISSUE 2
February
2010

Structure, thermal and magnetic properties of $Fe_{43}Co_{14}Ni_{14}B_{20}Si_5Nb_4$ bulk metallic glass

R. Nowosielski [a], R. Babilas [a,*], S. Griner [a], T. Czeppe [b]
[a] Division of Nanocrystalline and Functional Materials and Sustainable Pro-ecological Technologies, Institute of Engineering Materials and Biomaterials, Silesian University of Technology, ul. Konarskiego 18a, 44-100 Gliwice, Poland
[b] Institute of Metallurgy and Materials Science, ul. W. Reymonta 25, 30-059 Kraków, Poland
* Corresponding author: E-mail address: rafal.babilas@polsl.pl

Received 10.12.2009; published in revised form 01.02.2010

Materials

ABSTRACT

Purpose: The paper presents structure characteristics, thermal stability and soft magnetic properties analysis of Fe-based bulk metallic glass in as-cast state and after crystallization process.
Design/methodology/approach: The studies were performed on $Fe_{43}Co_{14}Ni_{14}B_{20}Si_5Nb_4$ metallic glass in a form of plates and rods. The amorphous structure of tested samples was examined by X-ray diffraction (XRD), transmission electron microscopy (TEM) and scanning electron microscopy (SEM) methods. The thermal stability of the glassy samples was measured using differential scanning calorimetry (DSC). The soft magnetic properties examination of tested material contained initial magnetic permeability and magnetic permeability relaxation measurements.
Findings: The XRD and TEM investigations revealed that the studied as-cast plates and rods were amorphous. Broad diffraction halo could be observed for all tested samples, indicating the formation of a glassy phase with the diameters up to 3 mm for rods. The fracture surface of rod samples appears to consist of two different zones which might correspond with different amorphous structures of studied materials. The thermal stability parameters of rod with diameter of 3 mm, such as glass transition temperature, onset crystallization temperature and supercooled liquid area were measured by DSC to be 797 K, 854 K, 57 K, respectively. The heat treatment process of rod samples involved in crystallization of α-Fe phase and formation of iron borides at temperature above 873 K.
Practical implications: The appropriate increase of annealing temperature significantly improved soft magnetic properties of examined alloy by increasing the initial magnetic permeability and decreasing the magnetic permeability relaxation.
Originality/value: The success of fabrication of studied Fe-based bulk metallic glass in a form of plates and rods is important for the future progress in research and practical application of those glassy materials.
Keywords: Amorphous materials; Bulk metallic glasses; Thermal stability; Soft magnetic properties

Reference to this paper should be given in the following way:
R. Nowosielski, R. Babilas, S. Griner, T. Czeppe, Structure, thermal and magnetic properties of $Fe_{43}Co_{14}Ni_{14}B_{20}Si_5Nb_4$ bulk metallic glass, Journal of Achievements in Materials and Manufacturing Engineering 38/2 (2010) 123-130.

1. Introduction

Iron-based metallic glasses have received great attention of researchers, because of their good magnetic, mechanical properties and corrosion resistance. Moreover, these alloys are potential candidates as precursor for nanocrystalline soft magnetic materials [1].

However, it is generally known that preparation of glassy materials requires high critical cooling rates of about 10^6 K/s. This condition largely limits the commercial applications of Fe-based amorphous materials because of the limitations of the sample size and shape, only to the wires or ribbons [2].

Inoue et al. succeeded in casting Fe-based bulk metallic glasses by copper mould casting in the following systems: Fe-(Al,Ga)-P-C-B-Si, Fe-(Zr,Hf,Nb,Ta)-B, Fe-(Co,Ni)-B-Si-Nb, Fe-(Cr,Mo)-B-C and Fe-Nd-Al. These systems alloys have good glass-forming ability and could be prepared in different bulk forms like rods, plates, discs and rings with low critical cooling rates below 10^3 K/s [3].

The Fe-based bulk metallic glasses with high glass-forming ability (GFA) should realize the empirical rules proposed by Inoue. These rules said that alloy with good GFA: (1) should have at least three components, two of which are metallic; (2) the alloy should contain two or more metallic elements with different atomic sizes and near-zero heats of mixing; (3) the metallic elements should have large negative heats of mixing with the metalloid type of components [4-6].

The work was succeeded in fabrication of $Fe_{43}Co_{14}Ni_{14}B_{20}Si_5Nb_4$ bulk metallic glass, which is classified for the Fe-(Co, Ni)-B-Si-Nb alloy system proposed by Inoue. This alloy seems to have good glass-forming ability, great thermal stability and good soft magnetic properties.

2. Material and research methodology

The aim of this paper is to characterize microstructure, thermal stability and soft magnetic properties analysis of $Fe_{43}Co_{14}Ni_{14}B_{20}Si_5Nb_4$ bulk amorphous alloy in as-cast state and after heat treatment processing. Investigations were done with the use of XRD, TEM, SEM, DSC and magnetic measurements methods.

The investigated material was cast in a form of plates (g) 0.5 thick and 1 mm and rods with diameter (ø) of 1.5, 2 and 3 mm. The ingot was prepared by induction melting of a mixture of pure elements of Fe, Co, Ni, Nb, Si and B under protective gas atmosphere.

Studied samples were manufactured by the pressure die casting method (Fig.1). The pressure die casting technology [7, 8] is the method of casting a molten alloy ingot in a copper mould under gas pressure. The chemical composition of the studied Fe-based metallic glass allows to cast this kind of material in bulk forms, however in this paper, the authors used samples in a form of plates and rods.

In order to study crystallization processes, rods, in as-cast state, were annealed at the temperature range from 373 K to 923 K at the step of 50 K. Tested samples were annealed in electric chamber furnace under protective argon atmosphere. The annealing time was constant and equalled to 1 hour.

Structure analysis of the samples in as-cast state was carried out using X-ray diffractometer (XRD) with $Co_{K\alpha}$ radiation for plate and rod samples examination. The data of diffraction lines were recorded by "step-scanning" method in 2θ range from 35° to 80°.

The fracture morphology of the rods with 1.5, 2 and 3 mm diameter was analyzed using the scanning electron microscopy (SEM).

Transmission electron microscopy (TEM) was used for the structural characterization of rods in as-cast state and after annealing procedure. Thin foils for TEM observation (from central part of the tested samples) were prepared by an electrolytic polishing method after previous mechanical grinding.

Thermal stability associated with glass transition (T_g), onset (T_x) and peak (T_p) crystallization temperatures, Curie temperature (T_c) and supercooled liquid area (ΔT_x) between T_g and T_x was examined by differential scanning calorimetry (DSC). The heating rate of calorimetry measurements, under argon protective atmosphere, was 20 K/min.

Magnetic measurements of annealed rods with diameter of 1.5 and 2 mm, carried at room temperature, included the following properties:

(a) relative magnetic permeability (μ_r) - determined by Maxwell-Wien bridge at the frequency of 1030 Hz and the magnetic field H= 0.5 A/m [9-12];

(b) magnetic permeability relaxation ($\Delta\mu/\mu$) also defined as "magnetic after-effects" - determined by measurement changes of the magnetic permeability as a function of time after demagnetization, where $\Delta\mu$ is a difference between the magnetic permeability determined at t_1 = 30 s and t_2 = 1800 s after demagnetization [13-15].

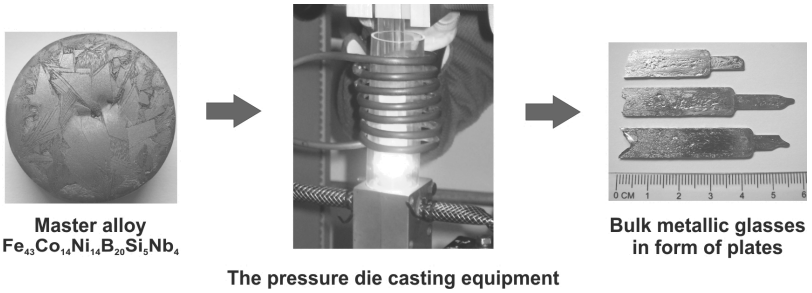

Fig. 1. Schematic illustration of the pressure die casting method used for bulk amorphous samples casting

3. Results and discussion

The X-ray diffraction investigations confirmed that the studied as-cast glassy samples were amorphous. The diffraction patterns of the tested plates 0.5 and 1 mm thick(Fig.2) and rods with diameter of 1.5, 2 and 3 mm (Fig.3) show the broad diffraction halo characteristic for the amorphous structure of glassy alloys.

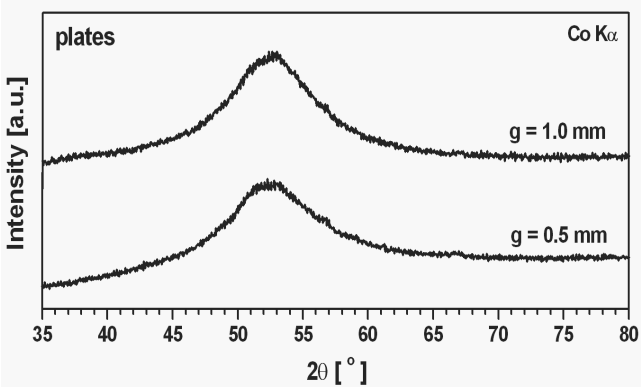

Fig. 2. X-ray diffraction patterns of $Fe_{43}Co_{14}Ni_{14}B_{20}Si_5Nb_4$ glassy plates in as-cast state of 0.5 and 1 mm tick

Figs. 4 and 5 present TEM images and electron diffraction patterns of the selected samples in as-cast state: plate with thickness of 0.5 mm and rod with diameter of 2 mm.

The TEM images revealed only some changes in contrast, which is characteristic for amorphous structure. The electron diffraction patterns consisted only of the halo rings. Broad diffraction halo can be seen for all tested samples, indicating the formation of a glassy phase.

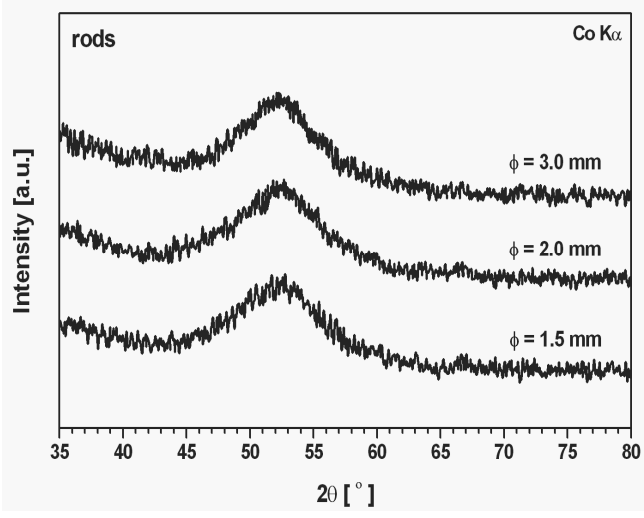

Fig. 3. X-ray diffraction patterns of $Fe_{43}Co_{14}Ni_{14}B_{20}Si_5Nb_4$ glassy rods in as-cast state with diameter 1.5, 2 and 3 mm

The good glass-forming ability enables casting of $Fe_{43}Co_{14}Ni_{14}B_{20}Si_5Nb_4$ bulk metallic glassy rod with a diameter of 3 mm. As it is believed, the reason for the large glass-forming ability results from three empirical rules formulated by Inoue [4-6].

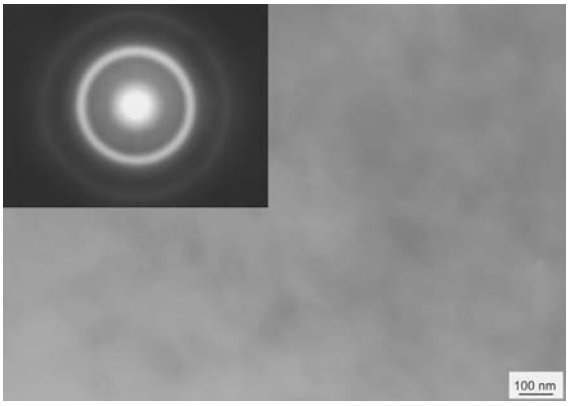

Fig. 4. Transmission electron micrograph and electron diffraction pattern of as-cast glassy $Fe_{43}Co_{14}Ni_{14}B_{20}Si_5Nb_4$ plate 0.5 mm thick

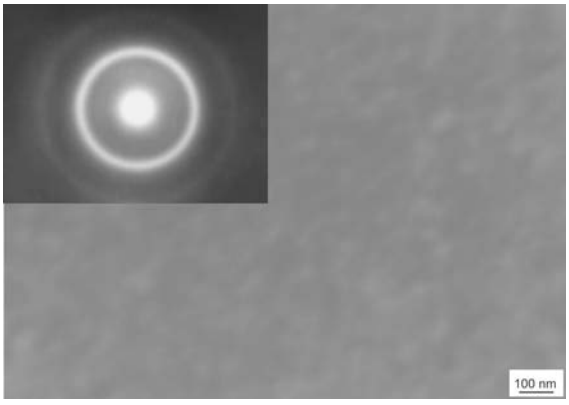

Fig. 5. Transmission electron micrograph and electron diffraction pattern of as-cast glassy $Fe_{43}Co_{14}Ni_{14}B_{20}Si_5Nb_4$ rod with diameter of 2 mm

The Fe-Si-B system, as the basic for the composition of Fe-Co-Ni-B-Si-Nb alloy realizes three empirical rules for good glass-forming ability. The addition of Co, Ni, and Nb in this alloy system supports the Inoue's rules concerning multicomponent alloy systems, consisting of more than three elements. The studied alloy consists of six elements. Moreover, it exists a significant difference in atomic size ratio among the main constituent elements. The sequence of atomic size goes as follows: Nb > Ni > Co > Fe > Si > B.

In Fig. 6 the DSC curves are shown measured at the rate of 20 K/min in as-cast state on amorphous plates 0.5 and 1 mm thick.

The exothermic peaks describing crystallization were observed for both samples in a form of plates. The crystallization effect for the plate sample 0.5 mm thick includes onset

crystallization temperature T_x = 849 K and peak crystallization temperature T_p = 873 K. In the case of the plate 1 mm thick, the exothermic effect includes onset of the crystallization temperature at T_x = 849 K and peak crystallization temperature at T_p = 872 K. The DSC analysis of the plates allowed to determine glass transition temperatures, which were 797 K and 800 K for samples 0.5 and 1 mm thick, respectively.

The DSC curves measured at the same rate on amorphous rods with of 1.5, 2 and 3 mm diameters, in as-cast state are shown in Fig. 7. Results of DSC investigations for rods confirmed that the peak crystallization temperature (T_p) increased while increasing the sample diameter. This may be the reason for the changes in the amorphous structure at the sample diameter increase.

For the rod with diameter of 3 mm, glass transition, onset crystallization temperature and supercooled liquid area were 797 K, 854 K and 57 K, respectively (Fig.7).

The DSC results also allow to determine Curie temperature (T_c) for the glassy rods. The Curie temperature of rod with diameter of 1.5 mm has a value of 604 K. For the sample with diameter of 2 mm, it was 602 K and for rod with diameter 3 mm 583 K, consequently (Fig.7).

The variation of the Curie temperature and crystallization temperature is probably also due to differences in the amorphous structures of the rods while increasing diameters.

The thermal stability parameters of studied glasses, glass transition temperature (T_g), onset crystallization temperature (T_x) and supercooled liquid area (ΔT_x) are presented in Table 1.

Table 1.
Thermal properties of the studied $Fe_{43}Co_{14}Ni_{14}B_{20}Si_5Nb_4$ samples in a form of plates and rods, in as-cast state

Sample	Thickness [mm]	T_g [K]	T_x [K]	ΔT_x [K]
Plate	0.5	797	849	52
	1	800	849	49
Rod	1.5	796	845	49
	2	791	845	54
	3	797	854	57

The appearance of the fracture surface of the investigated samples in a form of rods was investigated by SEM at different magnifications. Figs. 8, 9 and 10 present micrographs of as-cast glassy rods with diameter of 1.5, 2 and 3 mm.

The fracture surfaces appear to consist of different fracture zones. The fractures could be classified as mixed types with indicated zones containing weakly formed of “river” and “shell” patterns (Zone I) and “smooth” areas (Zone II). The “river” patterns are characteristic for metallic glassy alloys. The fracture surface of rod samples appears to consist of two different zones, which probably inform about different amorphous structures of the studied samples.

In order to investigate the crystallized phases the $Fe_{43}Co_{14}Ni_{14}B_{20}Si_5Nb_4$ bulk metallic glass in a form of the rod (ø = 1.5 mm) was annealed under protective atmosphere. The TEM examinations confirmed the formation of the single crystals in samples after annealing at temperature of 823 K. In Figs. 11, 12 and 13 TEM micrographs, electron diffraction patterns and its solutions are presented, for samples annealed at 823 K, 873 K and 923 K.

Annealing at temperature from 823 K to 923 K obviously causes formation of the crystalline phases. The phase analysis performed from the electron diffraction patterns enables the identification of α-Fe phase and iron borides - Fe_3B. The crystallization process consisted of the primary crystallization of α-Fe phase followed by the formation of iron borides.

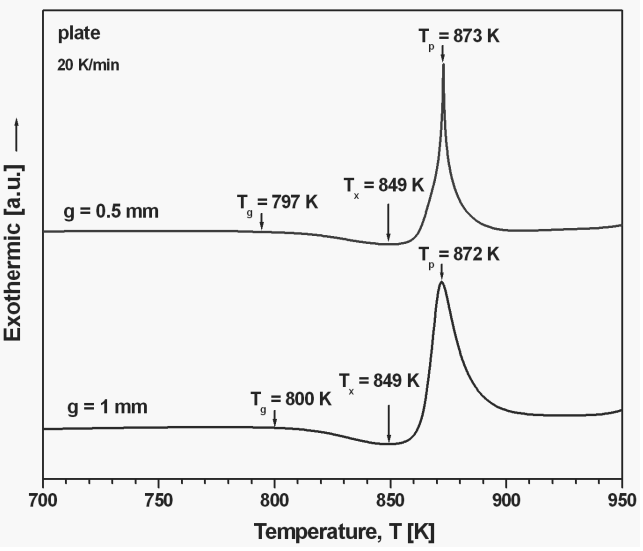

Fig. 6. DSC curves of $Fe_{43}Co_{14}Ni_{14}B_{20}Si_5Nb_4$ glassy alloy plates in as-cast state (heating rate 20 K/min)

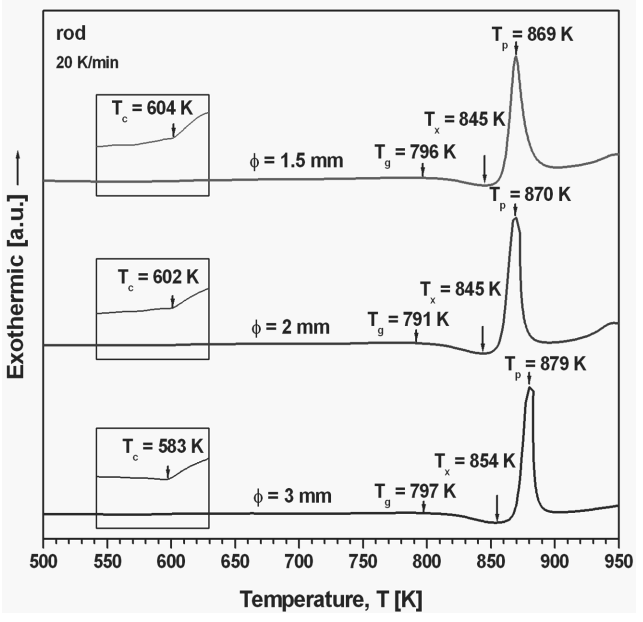

Fig. 7. DSC curves of $Fe_{43}Co_{14}Ni_{14}B_{20}Si_5Nb_4$ glassy alloy rods in as-cast state (heating rate 20 K/min)

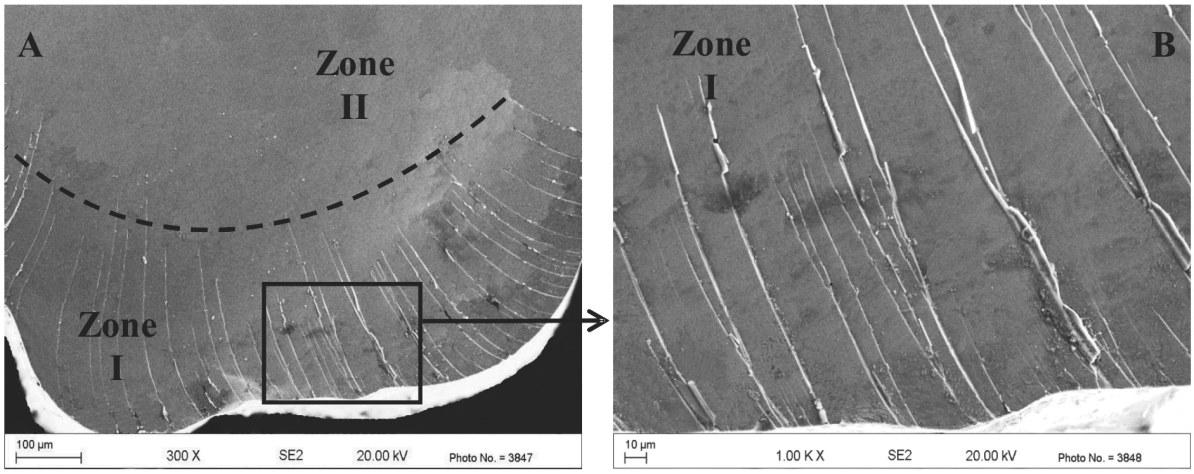

Fig. 8. SEM micrographs of the fracture morphology of $Fe_{43}Co_{14}Ni_{14}B_{20}Si_5Nb_4$ amorphous rod in as-cast state with diameter of 1.5 mm: A – magn. 300x, B – magn. 1000x

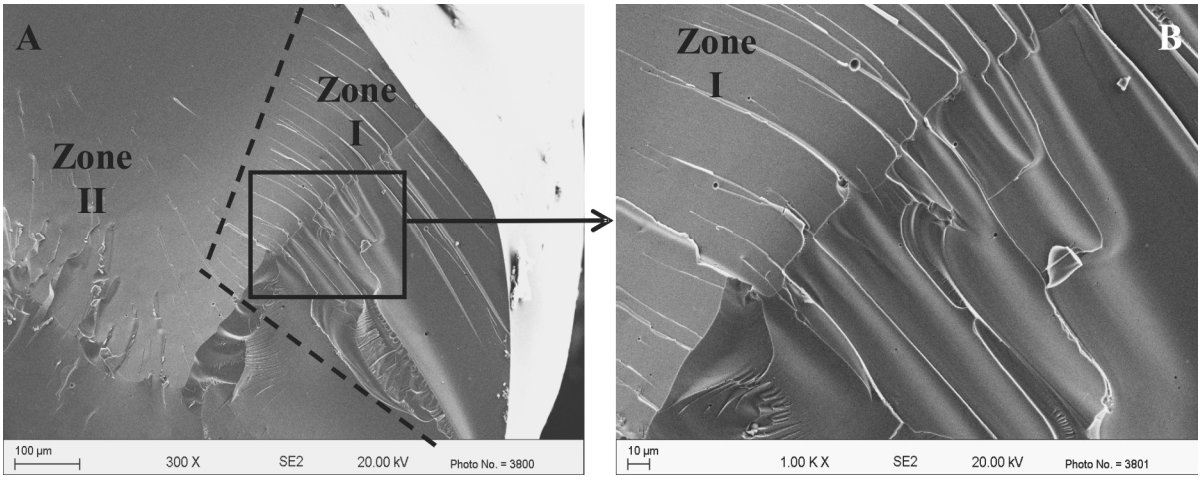

Fig. 9. SEM micrographs of the fracture morphology of $Fe_{43}Co_{14}Ni_{14}B_{20}Si_5Nb_4$ amorphous rod in as-cast state with diameter of 2 mm: A – magn. 300x, B – magn. 1000x

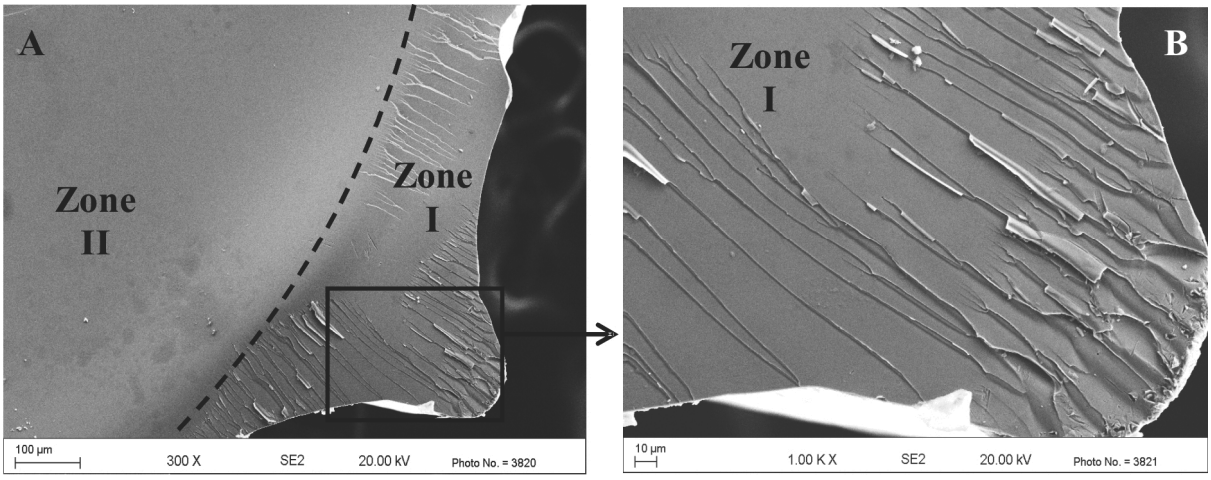

Fig. 10. SEM micrographs of the fracture morphology of $Fe_{43}Co_{14}Ni_{14}B_{20}Si_5Nb_4$ amorphous rod in as-cast state with diameter of 3 mm: A – magn. 300x, B – magn. 1000x

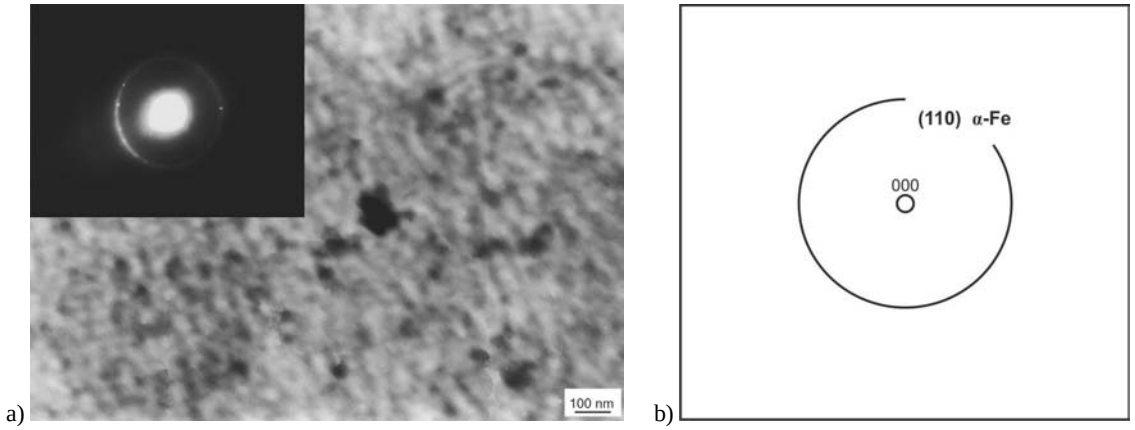

Fig. 11. Transmission electron micrograph plus electron diffraction pattern (a) and the solution of diffraction pattern (b) of $Fe_{43}Co_{14}Ni_{14}B_{20}Si_5Nb_4$ alloy in a form of rod (ø = 1.5 mm) after annealing at 823 K for 1 hour

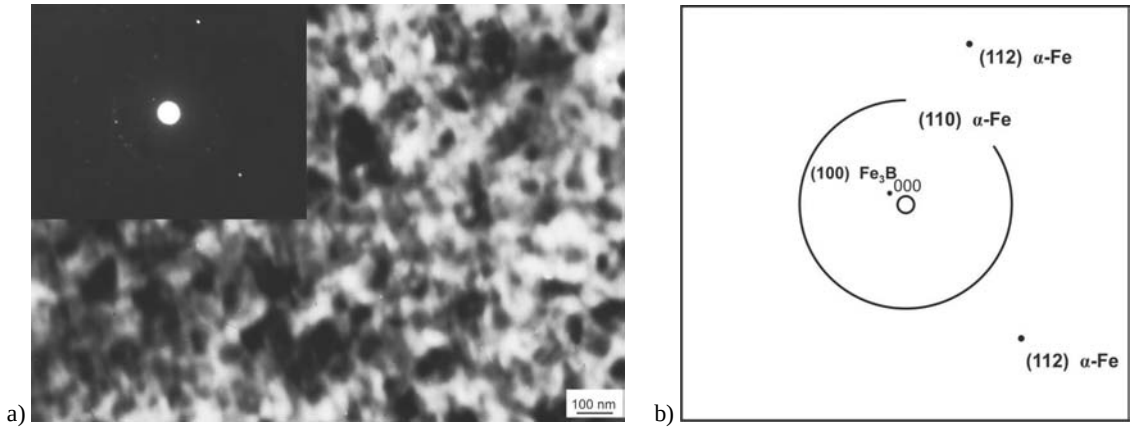

Fig. 12. Transmission electron micrograph plus electron diffraction pattern (a) and the solution of diffraction pattern (b) of $Fe_{43}Co_{14}Ni_{14}B_{20}Si_5Nb_4$ alloy in a form of rod (ø = 1.5 mm) after annealing at 873 K for 1 hour

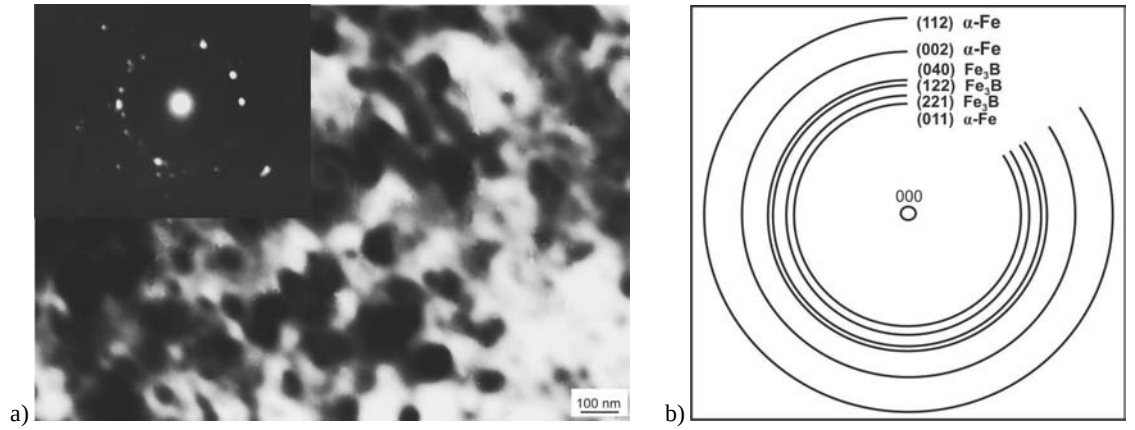

Fig. 13. Transmission electron micrograph plus electron diffraction pattern (a) and the solution of diffraction pattern (b) of $Fe_{43}Co_{14}Ni_{14}B_{20}Si_5Nb_4$ alloy in a form of rod (ø = 1.5 mm) after annealing at 923 K for 1 hour

The initial magnetic permeability (μ_r) for rods with diameter of 1.5 and 2 mm determined at room temperature versus annealing temperature (T_a) is shown in Fig. 14. The initial magnetic permeability of the examined samples increases along with the increase of annealing temperature and reaches a distinct maximum at 823 K, similarly to rods with remaining diameters. The temperature of annealing process, which corresponds to the maximum of initial magnetic permeability (μ_{rmax} = 1127 for ø = 1.5 mm and μ_{rmax} = 780 for ø = 2 mm) may be defined as the optimisation of the annealing temperature (T_{op}).

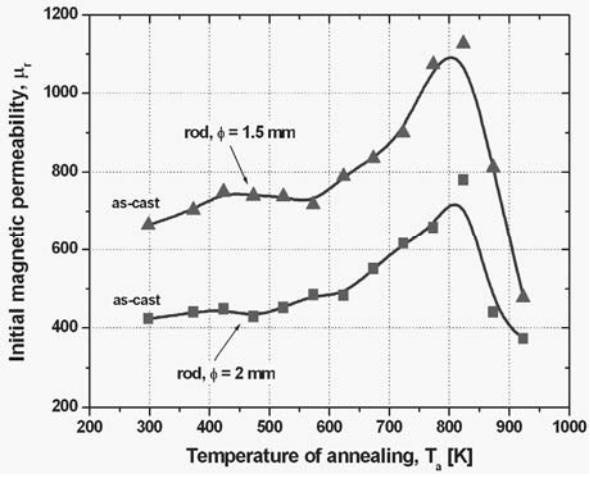

Fig. 14. Initial magnetic permeability of $Fe_{43}Co_{14}Ni_{14}B_{20}Si_5Nb_4$ alloy in a form of the rods, determined at room temperature versus annealing temperature

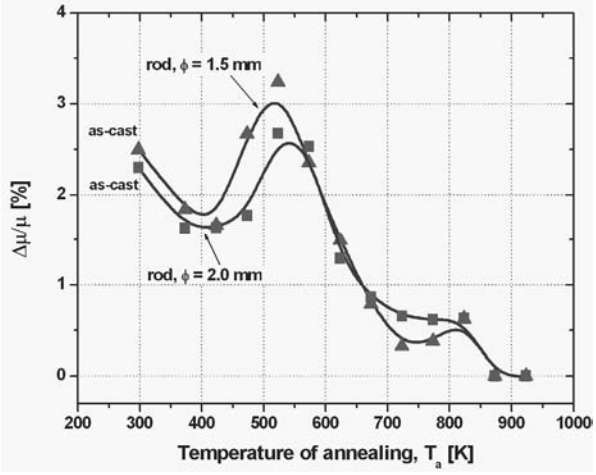

Fig. 15. Magnetic permeability relaxation of $Fe_{43}Co_{14}Ni_{14}B_{20}Si_5Nb_4$ alloy in from of the rods, determined at room temperature versus annealing temperature

The magnetic permeability relaxation of the tested rods in relation to annealing temperature is shown in Fig. 15. Basing on the literature [1, 13-15], the intensity of $\Delta\mu/\mu$ is directly proportional to the concentration of the defects in amorphous materials, i.e. free volume concentration. The value of $\Delta\mu/\mu$ increases in the temperature range from 423 K to 523 K, for the rods with diameters of 1.5 and 2 mm, respectively.

Table 2.
Magnetic properties of studied $Fe_{43}Co_{14}Ni_{14}B_{20}Si_5Nb_4$ alloy annealing at optimized temperature (T_{op})

Sample	ø [mm]	T_{op} [K]	μ_r	$\Delta\mu/\mu$ [%]
Rod	1.5	823	1127	0.6
	2	823	780	0.6

At temperatures higher than 523 K, the successive increase of annealing temperature causes the decrease of $\Delta\mu/\mu$ for the samples with diameters of 1.5 and 2 mm, respectively. It is significant that the optimized annealing temperature (T_{op}) corresponds to the decrease of the magnetic instability ($\Delta\mu/\mu$). This means that the optimisation annealing reduces time instabilities (free volume) of the magnetic permeability.

Finally, Figs. 14 and 15 present values of μ_r and $\Delta\mu/\mu$ in as-cast state for the examined rods. Distinct differences in the initial magnetic permeability between rods with diameter 1.5 and 2 mm could be explained by the different amorphous structure.

Table 2 summarises information concerning magnetic properties of the studied alloy in a form of the rods with diameters 1.5 and 2 mm after annealing at optimized temperature (T_{op}).

4. Conclusions

The investigations performed on the different samples of the $Fe_{43}Co_{14}Ni_{14}B_{20}Si_5Nb_4$ bulk metallic glass allowed to formulate the following statements:

- the XRD and TEM investigations revealed that the studied as-cast bulk glassy samples (plates and rods) were amorphous,
- the SEM images showed that studied fractures of rods in as-cast state indicated two structurally different zones,
- changes of Curie temperature, crystallisation temperature and glass transition temperature versus the thickness of the glassy samples (different cooling rates) were stated,
- the thermal stability parameters of rod with diameter of 3 mm, such as T_g, T_x and ΔT_x were measured to be 797 K, 854 K, 57 K, respectively
- the annealing treatment caused the formation of the α-Fe and iron borides crystalline phases at temperature above 873 K,
- the initial magnetic permeability increased together with the increase of annealing temperature and reached the distinct maximum at 823 K for rods with diameter of 1.5 and 2 mm,
- optimized annealing temperature (T_{op}) is connected with the significant decrease in magnetic instability ($\Delta\mu/\mu$),
- success in preparation of the studied Fe-based bulk metallic glass, in a form of the plates and rods is important for the future progress in research and practical application.

Acknowledgements

The authors would like to thank Dr W. Głuchowski (Non-Ferrous Metals Institute, Gliwice) and Dr Z. Stokłosa (Institute of Materials Science, University of Silesia, Katowice) for a cooperation and helpful comments.

References

[1] J. Rasek, Some diffusion phenomena in crystalline and amorphous metals, Silesian University Press, Katowice, 2000 (in Polish).
[2] D.Y. Liu, W.S. Sun, A.M. Wang, H.F. Zhang, Z.Q. Hu, Preparation, thermal stability, and magnetic properties of Fe-Co-Zr-Mo-W-B bulk metallic glass, Journal of Alloys and Compounds 370 (2004) 249-253.
[3] A. Inoue, B.L. Shen, C.T. Chang, Fe- and Co-based bulk glassy alloys with ultrahigh strength of over 4000 MPa, Intermetallics 14 (2006) 936-944.
[4] A. Inoue, Stabilization of supercooled liquid and opening-up of bulk glassy alloys, Proceedings of the Japan Academy 73 B (1997) 19-24.
[5] A. Inoue, A. Takeuchi, T. Zhang, Ferromagnetic bulk amorphous alloys, Metallurgical and Materials Transactions A 29A (1998) 1779-1793
[6] A. Inoue, A. Makino, T. Mizushima, Ferromagnetic bulk glassy alloys, Journal of Magnetism and Magnetic Materials 215-216 (2000) 246-252.
[7] R. Nowosielski, R. Babilas, Structure and magnetic properties of $Fe_{36}Co_{36}B_{19}Si_5Nb_4$ bulk metallic glasses, Journal of Achievements in Materials and Manufacturing Engineering 30/2 (2008) 135-140.
[8] R. Nowosielski, R. Babilas, S. Griner, Z. Stokłosa, Structure and soft magnetic properties of $Fe_{72}B_{20}Si_4Nb_4$ bulk metallic glasses, Archives of Materials Science and Engineering 35/1 (2009) 13-20.
[9] R. Nowosielski, R. Babilas, S. Griner, G. Dercz, A. Hanc, Crystallization of $Fe_{72}B_{20}Si_4Nb_4$ metallic glasses ribbons, Journal of Achievements in Materials and Manufacturing Engineering 34/1 (2009) 15-22.
[10] D. Szewieczek, T. Raszka, Structure and magnetic properties of $Fe_{63.5}Co_{10}Cu_1Nb_3Si_{13.5}B_9$ alloy, Journal of Achievements in Materials and Manufacturing Engineering 19 (2006) 179-182.
[11] D. Szewieczek, T. Raszka, J. Olszewski, Optimisation the magnetic properties of the $(Fe_{1-x}Co_x)_{73.5}Cu_1Nb_3Si_{13.5}B_9$ (x=10; 30; 40) alloys, Journal of Achievements in Materials and Manufacturing Engineering 20 (2007) 31-36.
[12] S. Lesz, D. Szewieczek, J.E. Frąckowiak, Structure and magnetic properties of amorphous and nanocrystalline $Fe_{85.4}Hf_{1.4}B_{13.2}$ alloy, Journal of Achievements in Materials and Manufacturing Engineering 19 (2006) 29-34.
[13] P. Kwapuliński, J. Rasek, Z. Stokłosa, G. Badura, B. Kostrubiec, G. Haneczok, Magnetic and mechanical properties in FeXSiB (X=Cu, Zr, Co) amorphous alloys, Archives of Materials Science and Engineering 31/1 (2008) 25-28.
[14] G. Badura, J. Rasek, Z. Stokłosa, P. Kwapuliński, G. Haneczok, J. Lelątko, L. Pająk, Soft magnetic properties enhancement effect and crystallization processes in $Fe_{78-x}Nb_xSi_{13}B_9$ (x = 0, 2, 4) amorphous alloys, Journal of Alloys and Compounds 436 (2007) 43-50.
[15] P. Kwapuliński, Z. Stokłosa, J. Rasek, G. Badura, G. Haneczok, L. Pająk, L. Lelątko, Influence of alloying additions and annealing time on magnetic properties in amorphous alloys based on iron, Journal of Magnetism and Magnetic Materials 320 (2008) 778-782.